AD-A070 963 TEXAS UNIV AT AUSTIN APPLIED RESEARCH LABS F/G 17/1
EXPERIMENTAL SUPERPOSITION OF ACOUSTIC FIELDS FOR DETECTION PER--ETC(U)
MAR 79 J A SHOOTER, M L GENTRY N00039-78-C-0307
UNCLASSIFIED ARL-TM-79-3 NL

| OF |
AD
A070963

END
DATE
FILMED
8 -79
DDC

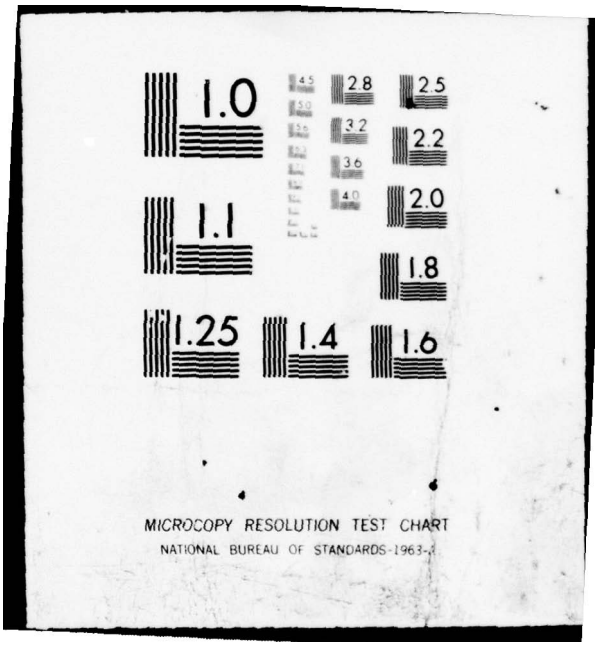
1.0
1.1
1.25
1.4
1.6
1.8
2.0
2.2
2.5
2.8
3.2
3.6
4.0
4.5
5.0
5.6
MICROCOPY RESOLUTION TEST CHART
NATIONAL BUREAU OF STANDARDS-1963-A

ARL-TM-79-3

LEVEL II

(10)

Copy No. 47

EXPERIMENTAL SUPERPOSITION OF ACOUSTIC FIELDS FOR DETECTION PERFORMANCE STUDIES

Jack A. Shooter
Milton L. Gentry, Jr.

APPLIED RESEARCH LABORATORIES
THE UNIVERSITY OF TEXAS AT AUSTIN
POST OFFICE BOX 8029, AUSTIN, TEXAS 78712

15 March 1979

Technical Memorandum

Prepared for:

NAVAL ELECTRONIC SYSTEMS COMMAND
DEPARTMENT OF THE NAVY
WASHINGTON, DC 20360

UNCLASSIFIED

SECURITY CLASSIFICATION OF THIS PAGE (When Date Entered)

REPORT DOCUMENTATION PAGE	READ INSTRUCTIONS BEFORE COMPLETING FORM
1. REPORT NUMBER	2. GOVT ACCESSION NO. / 3. RECIPIENT'S CATALOG NUMBER
4. TITLE (and Subtitle): EXPERIMENTAL SUPERPOSITION OF ACOUSTIC FIELDS FOR DETECTION PERFORMANCE STUDIES	5. TYPE OF REPORT & PERIOD COVERED: technical memorandum
	6. PERFORMING ORG. REPORT NUMBER: ARL-TM-79-3
7. AUTHOR(s): Jack A. Shooter; Milton L. Gentry, Jr.	8. CONTRACT OR GRANT NUMBER(s): N00039-78-C-0307
9. PERFORMING ORGANIZATION NAME AND ADDRESS: Applied Research Laboratories, The University of Texas at Austin, Austin, Texas 78712	10. PROGRAM ELEMENT, PROJECT, TASK AREA & WORK UNIT NUMBERS: 34 p.
11. CONTROLLING OFFICE NAME AND ADDRESS: Naval Electronic Systems Command, Department of the Navy, Washington, DC 20360	12. REPORT DATE: 15 March 1979
	13. NUMBER OF PAGES: 33
14. MONITORING AGENCY NAME & ADDRESS (if different from Controlling Office)	15. SECURITY CLASS. (of this report): UNCLASSIFIED
	15a. DECLASSIFICATION/DOWNGRADING SCHEDULE: N/A

16. DISTRIBUTION STATEMENT (of this Report)

Distribution limited to U.S. Government agencies only; TEST AND EVALUATION; 15 March 1979. Other requests for this document should be referred to NAVAL ELECTRONIC SYSTEMS COMMAND, PME 124-30.

17. DISTRIBUTION STATEMENT (of the abstract entered in Block 20, if different from Report)

18. SUPPLEMENTARY NOTES

19. KEY WORDS (Continue on reverse side if necessary and identify by block number)

superposition

404 434 GW

20. ABSTRACT (Continue on reverse side if necessary and identify by block number)

(U) The concept of superimposing a target acoustic field onto an independent noise acoustic field is discussed and sample results are presented using data from the deep Atlantic Ocean. The purpose is to explore the principles and methods of how this concept can be implemented for assessing signal detection in the presence of noise as applied to particular systems. The target signal was composed of high and low level components which were used simultaneously. From these data, the high level signal was —over

DD FORM 1 JAN 73 1473 EDITION OF 1 NOV 65 IS OBSOLETE

UNCLASSIFIED

SECURITY CLASSIFICATION OF THIS PAGE (When Data Entered)

20. Cont'd.

scaled down in amplitude and reinserted into the noise spectrum. The detection results of the actual low level signal and the reconstructed low level signal are compared and the results are shown to be essentially the same.

TABLE OF CONTENTS

LIST OF FIGURES

LIST OF TABLES

I. INTRODUCTION

This memorandum will discuss the concept of superimposing a target acoustic field onto an independent noise acoustic field and will present some example results using data from the deep Atlantic Ocean.[1] The purpose is to explore the principles and methods of how this concept can be implemented for assessing signal detection in the presence of noise as applied to particular systems. Section II will outline the general problem and provide the motivation for the superpositional approach to the solution. Section III will discuss the principle of superposition for a point receiver and an array of point receivers. Section IV will present experimental results where high and low level signals were used simultaneously. From these data, the high level signal was scaled down in amplitude and reinserted into the noise spectrum. The detection results of the actual low level signal and the reconstructed low level signal are compared and the results are shown to be essentially the same.

II. GENERAL PROBLEM

An acceptable procedure for assessing how well a system can detect a target signal in a noise field is to test it in a real environment over an extended period under many signal and noise conditions. This can be very expensive over an extended period of time and the environmental conditions will not always meet the specified noise conditions. The most serious problem is the general nonstationary aspect of the noise field which creates an interpretation problem in the case of a range changing source. That is, level changes in the noise field will change the signal-to-noise ratio (S/N) at the same time the signal level changes due to changing signal-receiver geometry. This means that S/N versus range and detection versus range must be very carefully assessed and interpreted in reference to the noise field. A second serious problem can be caused by the noise from a ship towing a target signal source, masking the ambient background noise. This means that in some cases, especially at short range, S/N measurements will not be signal to ambient background noise, but instead will be signal to tow ship noise.

It is proposed that a way of circumventing these problems is to record the signal and noise fields independently under field conditions. Because of the importance of boundary conditions and changes in a time varying environment, it cannot be overemphasized that the signal and noise fields must be recorded at the same site and position. It is further emphasized that the signal field repeatability should be tested to establish confidence in the stability of the final results. A second emphasis is

placed on recording the noise field over a time sufficient to measure different noise conditions. For example, it has been shown that typical noise decorrelation times in the Atlantic Ocean and Mediterranean Sea are near 10 h in the shipping frequency band of the spectrum and a maximum of 25 h in the wind dominated part of the spectrum.[1] This means that, on the average, it is desirable to have 10×25 h or 10 days worth of noise recording to cover different levels of the noise field.

III. SUPERPOSITION

This section will briefly discuss the principle of superposition and describe a procedure that may be applied to superimpose real data recorded from an omnidirectional sensor and an array of sensors.

The principle of superposition is well known and discussed in every textbook on acoustics. Most solutions to the wave equation assume linear propagation and separate the solution into its components (e.g., modes) and build a complete solution by the principle of superposition. In effect most signal processing analyses assume linear systems and separate the acoustic field into its components (e.g., multiple source signals plus multiple noise sources) for ease of manipulation.

The basic assumption is that the acoustic pressure field at a point in space is the sum of pressure generated from multiple independent sources. Therefore they may be treated independently. In this case we want to record a high level signal field and sum it into one or more noise fields at different relative levels. Once again it is emphasized that this must be done with in situ real data because of the importance of boundaries and the many paths that a signal can take to arrive at a point. That is, computer simulated data would not be acceptable. In principle the recorded data to be scaled and summed can be in analog or digital form. Because of the experience and background of Applied Research Laboratories, The University of Texas at Austin (ARL:UT), in digital signal processing, the digital processing techniques would be the easiest and most accurate to implement.

The most straightforward example is in the case of a single omni sensor. In the case of independent signal and noise fields, the data can be processed independently before detection. That is, the signal spectra

and noise spectra can be computed independently and stored on magnetic tape, just as the standard ARL:UT AN/cw processor currently operates on data. The superposition then takes place in the frequency domain by scaling the signal spectrum to match a desired source level and summing onto a noise spectrum chosen to represent a particular noise condition. This is described in the following set of simple equations.

Let s be the received signal from a known source of known level and position and let n be an independent noise sample received by the same sensor in the same position but at a different time. The summed field is shown in Eq. (1) where the signal field is scaled by a.

$$x(t) = as(t) + n(t) \quad . \tag{1}$$

It is possible to make this sum directly in the time domain given the sampled time series s and n. However, the most costly and time consuming part of the ARL:UT processing is in the FFT time. If the sum is to be repeated for several values of a corresponding to different source levels and also repeated for different noise fields, then it would be far more efficient if the FFT's had to be done only once. It can be shown that it is necessary to do the FFT's only once for a specified set of parameters giving frequency resolution and averaging times (ALI's) by Fourier transforming Eq. (1) and forming the ensemble average of the resulting power spectra. Let $X(\omega)$ be the complex Fourier transform of $x(t)$ in Eq. (1), $S(\omega)$ be the transform of $s(t)$, and $N(\omega)$ be the transform of $n(t)$. Then the Fourier transform of Eq. (1) becomes

$$X(\omega) = aS(\omega) + N(\omega), \tag{2}$$

and the energy spectrum of Eq. (2) becomes

$$X(\omega)X^*(\omega) = a^2S(\omega)\ S^*(\omega) + N(\omega)N^*(\omega) + S(\omega)N^*(\omega) + N(\omega)S^*(\omega). \quad (3)$$

The ensemble average of Eq. (3) is

$$\langle XX^* \rangle = a^2\langle SS^* \rangle + \langle NN^* \rangle, \quad (4)$$

where

$$\langle SN^* \rangle = \langle NS^* \rangle = 0,$$

because S and N are independent and zero biased in time and frequency. Therefore Eq. (4) means that the signal and noise fields can be processed separately into spectra and stored, e.g., on tape, for postprocessing, using whatever scale factor a^2 is desired. For example, the postprocessing might involve frequency detection and line tracking as part of the signal classification.

The next case to be considered is that of an array of sensors to accomplish spatial processing. In this case each sensor can be treated independently in the time domain by sampling the signal and noise fields at different times, storing the time series, scaling the signal field, summing, and then forming beams in the frequency domain. Once again this technique is inefficient if a parameter study is to be done because of the number of times the beamforming and FFT process would have to be redone. Fortunately the same principle used in the single omnidirectional case can be applied to an array. This means that the signal field and noise fields can be processed independently and stored in the form of complex cross-spectral matrices, and the matrices can be later summed

using different scaling factors a. This can easily be shown to be valid by considering that, in spatial processing, the spatial information is contained in the differences between elements.[2] Therefore it is necessary to consider only the i and j elements in an array, as shown in Eq. (5).

$$x_i(t) = s_i(t) + n_i(t) \quad . \tag{5}$$

$$x_j(t) = s_j(t) + n_j(t) \quad .$$

This represents the superposition of the S and N fields at spatial points "i" and "j". The Fourier transform of Eq. (5) is

$$X_i(\omega) = S_i(\omega) + N_i(\omega)$$

$$X_j(\omega) = S_j(\omega) + N_j(\omega) \quad , \tag{6}$$

and the cross-spectra between i and j is seen in Eq. (7).

$$X_i X_j^* = S_i S_j^* + S_i N_j^* + N_i S_j^* + N_i N_j^* \quad . \tag{7}$$

The ensemble average of Eq. (7) is

$$\langle X_i X_j^* \rangle = \langle S_i S_j^* \rangle + \langle N_i N_j^* \rangle, \tag{8}$$

where

$$\langle S_i N_j^* \rangle = \langle N_i S_j^* \rangle = 0.$$

This means that, for independent signal and noise fields, the data can be processed independently into cross-spectral matrices which contain all information necessary for beamforming. Scaling and superposition can be applied to the matrices directly. In the case of a line array, the matrices

can be further compressed for data storage by averaging the diagonal elements (complex) and storing only those terms, which may be called the spatial correlation samples. Given the summed or superimposed matrices the post-processing can then form beams and do signal detection and tracking as in a normal processor.

IV. EXPERIMENTAL TEST ON OMNI DATA

A test of the theory outlined in section III was implemented using archived data from the deep Atlantic Ocean. In this exercise a cw source that generated high and low level signals simultaneously was used. The generated signals were the frequency pairs 70 Hz, 68 Hz and 156 Hz, 160 Hz and they were collocated. Collocation is especially important in data interpretation and analysis. It is well known that slight variations in source receiver geometry (e.g., source depth variations) will cause large fluctuations in signal level. The fact that they were collocated removes the effects of geometry between the high and low level signals.

The data were recorded by the omnidirectional hydrophones on an ACODAC and reduced to 5 min average spectra at a frequency resolution of 0.073 Hz. The archived spectra were then used to experimentally test the detection differences between an actual low level signal and a reconstructed low level signal. In this case the high level signal was scaled down and shifted in frequency before it was summed back into the noise field. In a real simulation exercise, where high level signals are to be used to reconstruct low level signals in a different noise field, the frequency shift would not be necessary. The advantage of these data is that the noise field is essentially the same for the real and synthesized signals, and the sources were collocated. Except for slight variations in noise because of different frequency bands, the differences in detection performance can be compared directly.

The experimental results here are limited to omnidirectional data. The theory in section III accounts for array processing but a definitive experimental test will have to be conducted at a later time.

The following sections discuss the details of the procedures used to obtain signal excess as a function of range for a real low level signal and a reconstructed low level signal.

A. A Method for Adjusting a High Level Signal

Given a power spectrum, i.e., a set of Fourier coefficients modulo squared, containing a high level cw signal, the first step in the procedure is to rescale those coefficients to correspond to the desired low level cw signal. The coefficients can then be added back into the spectrum in another band.

For example, suppose $\{C_\nu\}_{\nu=i}^{i+j}$ are the ith through i+jth FFT coefficients of a band containing a signal. The signal contained within this band can be scaled by "a" and moved to another band, $\{C_\nu\}_{\nu=k}^{k+j}$ by this simple process:

$$C_\nu = C_\nu + a^2 C_{i+\nu-k} \quad \text{for } \nu = k, k+1, \ldots, k+j. \tag{9}$$

The effect is to change the level of the signal by

$$\Delta SL = 10 \log a^2 \tag{10}$$

and to shift the signal to another frequency. In the data chosen, the noise carried along in the signal band will be scaled down by the same amount a^2, and when it is summed back into the spectrum it will have negligible effects.

B. The Experiment

The experiment performed was to take high level cw signals that were transmitted during the exercise and scale them to

the levels of actual low level signals that were being simultaneously transmitted. In particular, 70 Hz and 160 Hz high level signals were transmitted simultaneously with low level 68 Hz and 156 Hz signals. The high level 70 Hz and 160 Hz signals were scaled and shifted to 66 Hz and 166 Hz, respectively. Comparisons of signal excess were made between the reconstructed 66 Hz and real 68 Hz signals as well as between the real 156 Hz and the reconstructed 166 Hz signals.

The spectra used for analysis were taken from two ACODAC hydrophones, No. 3 and No. 6. Hydrophone 3 was at a depth of 4750 m, which corresponded to critical depth. Hydrophone 6 was at the bottom, or a depth of 5250 m.

The spectra were 5 min averages with a frequency range from 0 to 300 Hz and a coefficient spacing of 0.073 Hz.

Data from two radial cw tows were utilized for the high frequency signals. Run 1 was a southwest run away from the ACODAC and Run 2 was a north-northeast run also away from the receiver. The low frequency data were taken from the second run only.

C. Data Processing

The actual data processing consisted of determining the adjustments to the high level signals; adjusting the high level signals; computing background noise level estimates, signal excesses, and signal levels for the various cw signals; and finally, displaying the results.

Rather than rely on absolute source levels it was decided that the significant parameters were the relative differences in source level between the high and low level signals. The adjustment to the high level

signal was estimated as the median difference in level between the high and low level source pairs. This was measured when the sources were close to the receiver (<20 km). An example of measured differences in received SPL is shown in Fig. 1.

Figure 1 is shown on a scale of 5 dB per increment. A scatter of 2 dB is due to variance in the noise estimates used to debias the signal level estimates. The additional variations are due to received level differences between the two frequencies. The adjustment for the 160 Hz source was found to be -15.0 dB for Run 1 and -14.5 dB for Run 2. The median level difference between the 70 Hz and 60 Hz sources was found to be -22.0 dB (only the second tow was used). The median difference in background noise levels between the 68 Hz and the 66 Hz signals was found to be 0.55 dB; thus the final adjustment to the 70 Hz signal was chosen to be -21.45 dB. This was done so that the signal excess plots of the 68 Hz and 66 Hz signals could be compared. The noise level differences between 156 Hz and 166 Hz were considerably smaller and were ignored.

With the adjustment determined, the high level 70 Hz and 160 Hz signals were reduced in level, shifted in frequency to 66 Hz and 166 Hz, respectively, and then superimposed back onto the spectrum.

The noise level N around a given cw signal was a percentile estimate based on the FFT coefficients contained in a 3.0 to 3.5 Hz wide band centered about the cw signal, deleting the coefficients contained in a 1 Hz band centered about the cw signal.

Coefficient sums around the peak of 1, 3, and 5 elements were found over the wide band as well as over a smaller 0.5 Hz wide band centered about the cw signal. When the center frequencies of the wide

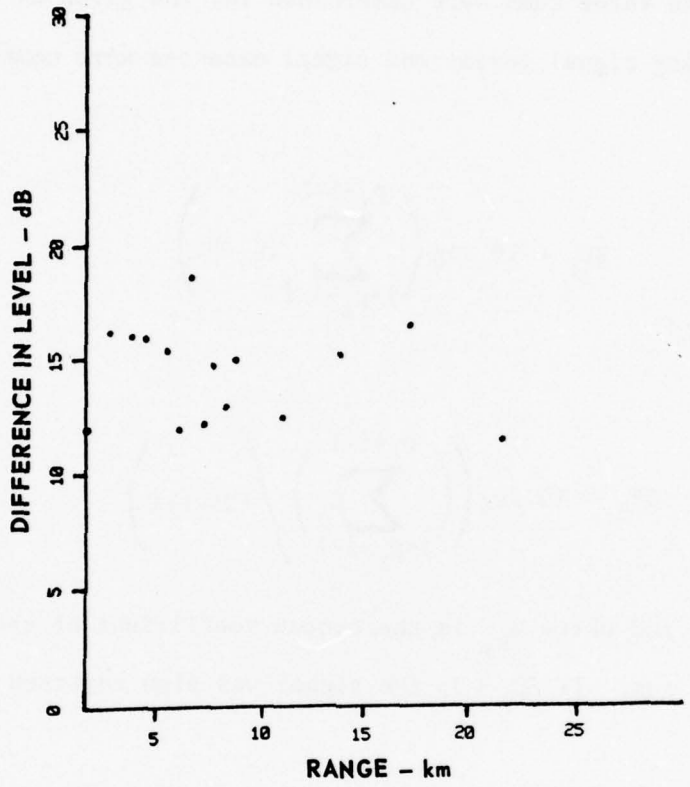

FIGURE 1
DIFFERENCE IN LEVEL BETWEEN THE 156 Hz cw SIGNAL AND THE 160 Hz cw SIGNAL ON HYDROPHONE 3 OVER THE FIRST RUN

ARL:UT
AS-79-427
JAS-GA
3-20-79

band peak sums were not the same as the center frequencies of the narrow-band peak sums, the signal was rejected as a false detection.

Once the three sums were determined for the given cw signal, three corresponding signal levels and signal excesses were computed as

$$SL_i = 10 \log\left(\sum_{j=p_i-i-1}^{p_i+i-1} (C_j - N)\right) , \qquad (11)$$

and

$$SE_i = 10 \log\left(\left(\sum_{j=p_i-i-1}^{p_i+i-1} C_j\right) \Big/ (2i-1)N\right) \qquad (12)$$

for i = 1, 2, 3, and where C_{p_i} is the center coefficient of the (2i-1) coefficient peak sum. If $SE_i < 0$, the signal was also rejected and SL_i was set to 0.

D. Results

The basic result was that the signal excess and the noise for the reconstructed and actual signals behave similarly when the plots are compared.

Figures 2 and 3 show three-dimensional spectra illustrating the insertion of a rescaled signal into a noise spectrum for the low frequency 66 Hz case and for the high frequency 166 Hz case. Both of these examples are for hydrophone 6 which was on the bottom. The signal excess is slightly higher on the bottom hydrophone because the noise for these data is slightly lower on the bottom hydrophone.

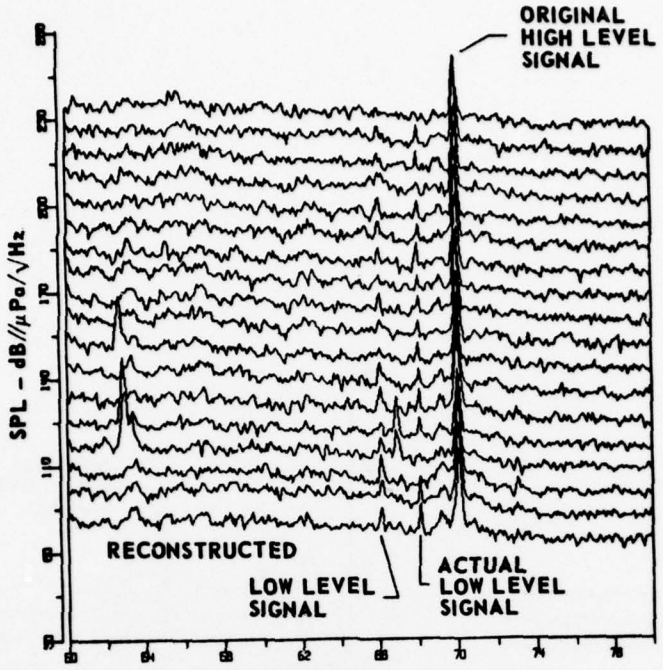

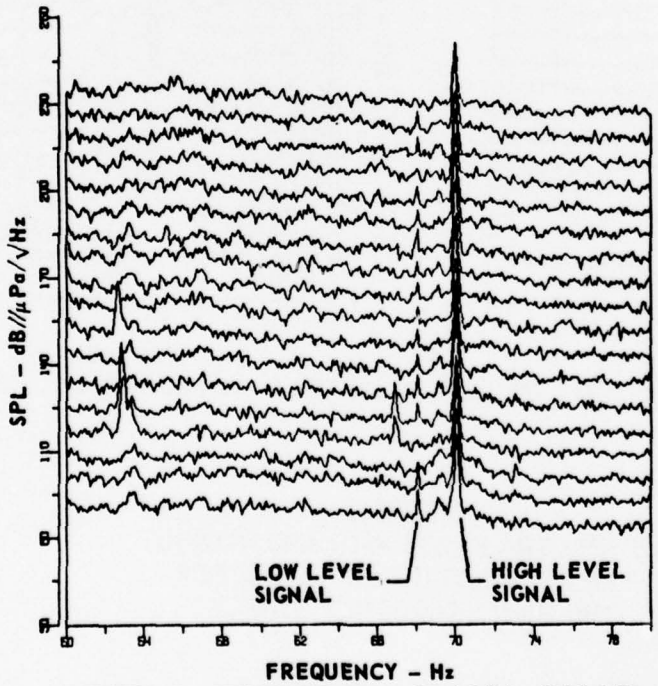

ARL:UT
AS-79-428
JAS - GA
3 - 20 - 79

FIGURE 2
3-D SPECTRA PLOTS WITH AND WITHOUT THE RECONSTRUCTED SIGNAL FOR THE LOW FREQUENCY SOURCES

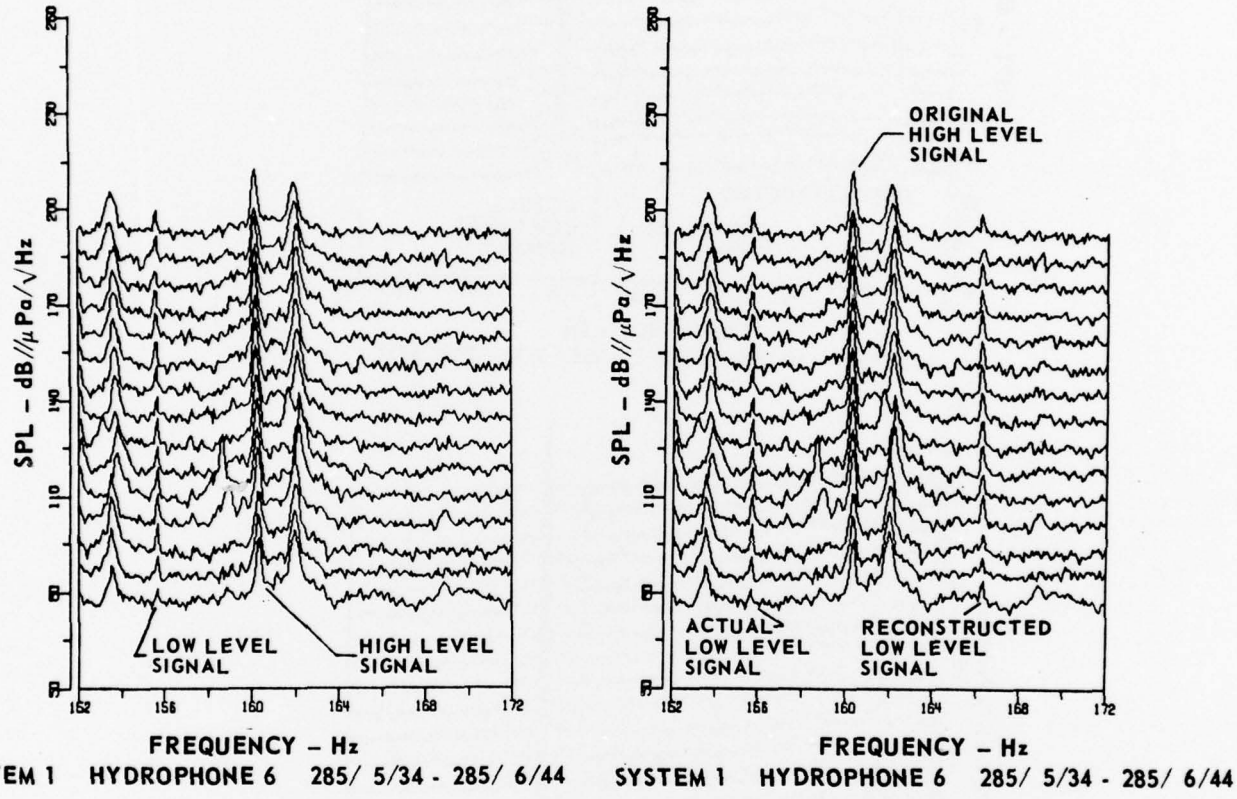

FIGURE 3
3-D SPECTRA PLOTS WITH AND WITHOUT THE RECONSTRUCTED SIGNAL FOR THE HIGH FREQUENCY SOURCES

ARL:UT
AS-79-429
JAS-GA
3-20-79

The salient points are in the figures showing the signal excess. Figure 4 shows signal excess for the critical depth receiver (HYD 3) and the bottom receiver (HYD 6) for the real (156 Hz) and reconstructed (166 Hz) signals. The signal excess as a function of range is on the average the same in all cases.

The details differ because of slight variations in the noise field. Please note that the noise scale in the figures is compressed 2:1 relative to the signal excess. Figure 5 shows signal excess for the same frequencies at a different time and it is noted that the noise is lower on the deeper receiver. Again the signal excess is the same, on the average, as a function of range for the real and reconstructed signals. The low frequency results are shown in Fig. 6; because of the higher noise level in this part of the spectrum, the signal excess is lower. However, the comparison of signal excess between the real and reconstructed signals is again the same.

The percentage of signals detected using the method discussed in section IV.C. tended to be higher for the reconstructed signal. The reconstructed signal detection percentages ranged from 35% to 88%, whereas the actual signal detection percentage ranged from 30% to 75%. The percent detections are summarized in Tables I and II. In this test the detection algorithm was a conservative estimator because it was designed to detect and measure cw propagation loss. A different algorithm could raise the probability of detection.

As a sensitivity study, the 166 Hz signal was simulated with adjustments of -14.5 dB, -15.0 dB, and -15.5 dB. The effect of the 0.5 dB perturbations in the 166 Hz level adjustment was simply to shift the

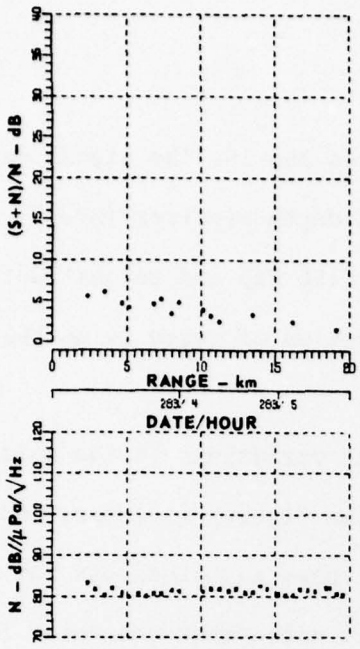

ACTUAL SIGNAL
HYDROPHONE 3

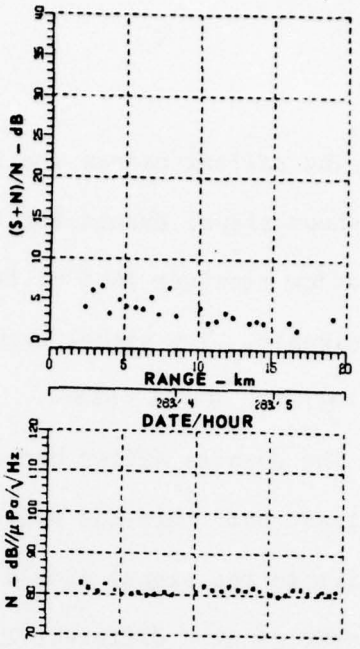

RECONSTRUCTED SIGNAL WITH
–15.0 dB ADJUSTMENT
HYDROPHONE 3

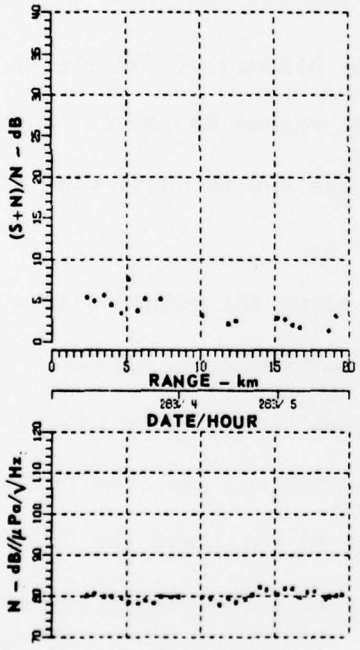

ACTUAL SIGNAL
HYDROPHONE 6
156 Hz

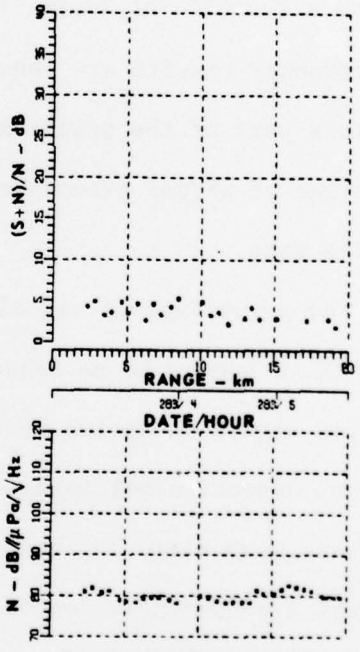

RECONSTRUCTED SIGNAL WITH
–15.0 dB ADJUSTMENT
HYDROPHONE 6
166 Hz

ARL:UT
AS-79-430
JAS-GA
3-20-79

FIGURE 4
SIGNAL EXCESS AND NOISE versus RANGE
FOR THE HIGH FREQUENCIES OVER RUN 1

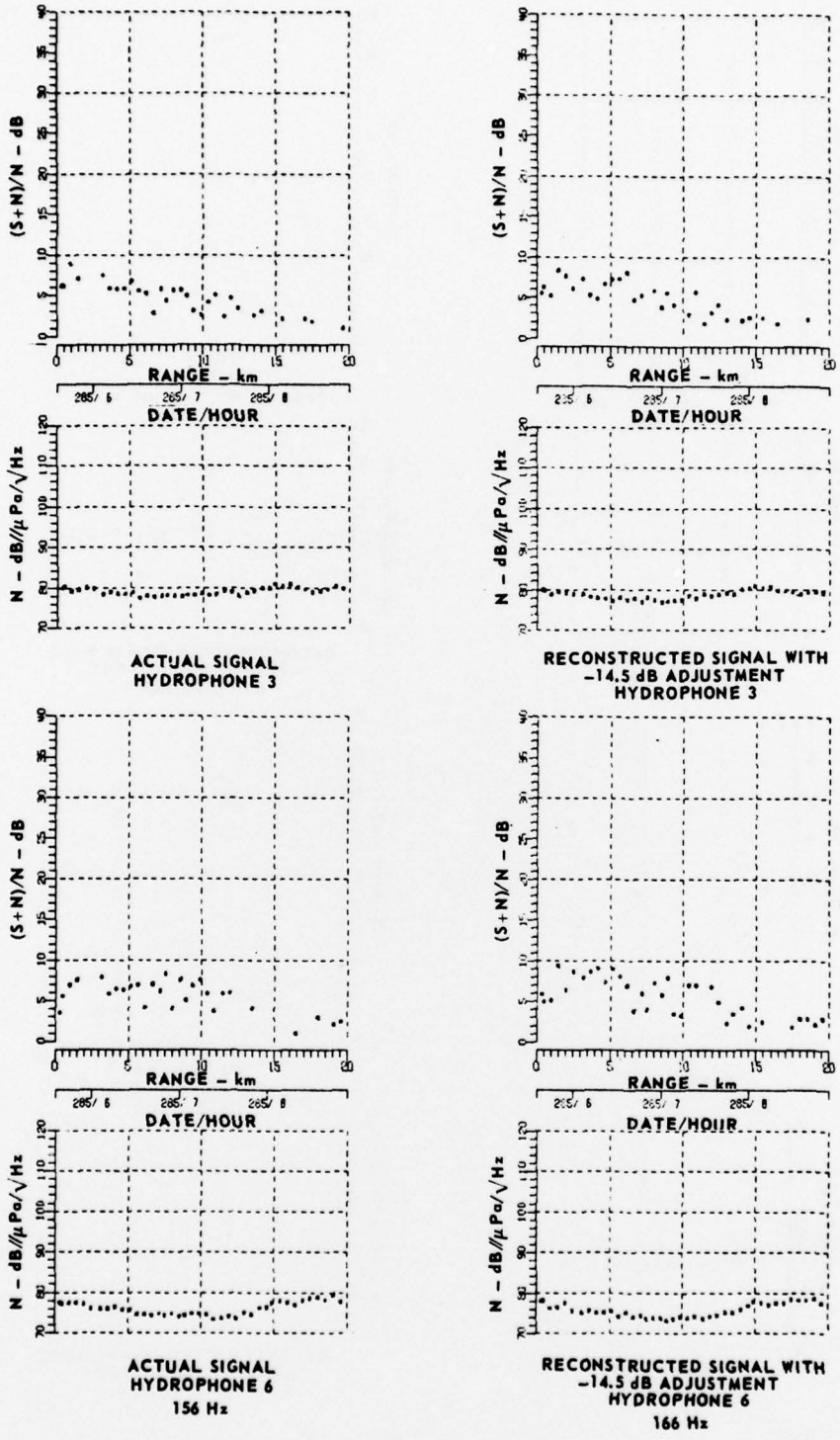

FIGURE 5
SIGNAL EXCESS AND NOISE versus RANGE
FOR THE HIGH FREQUENCIES OVER RUN 2

ARL:UT
AS-79-431
JAS-GA
3-20-79

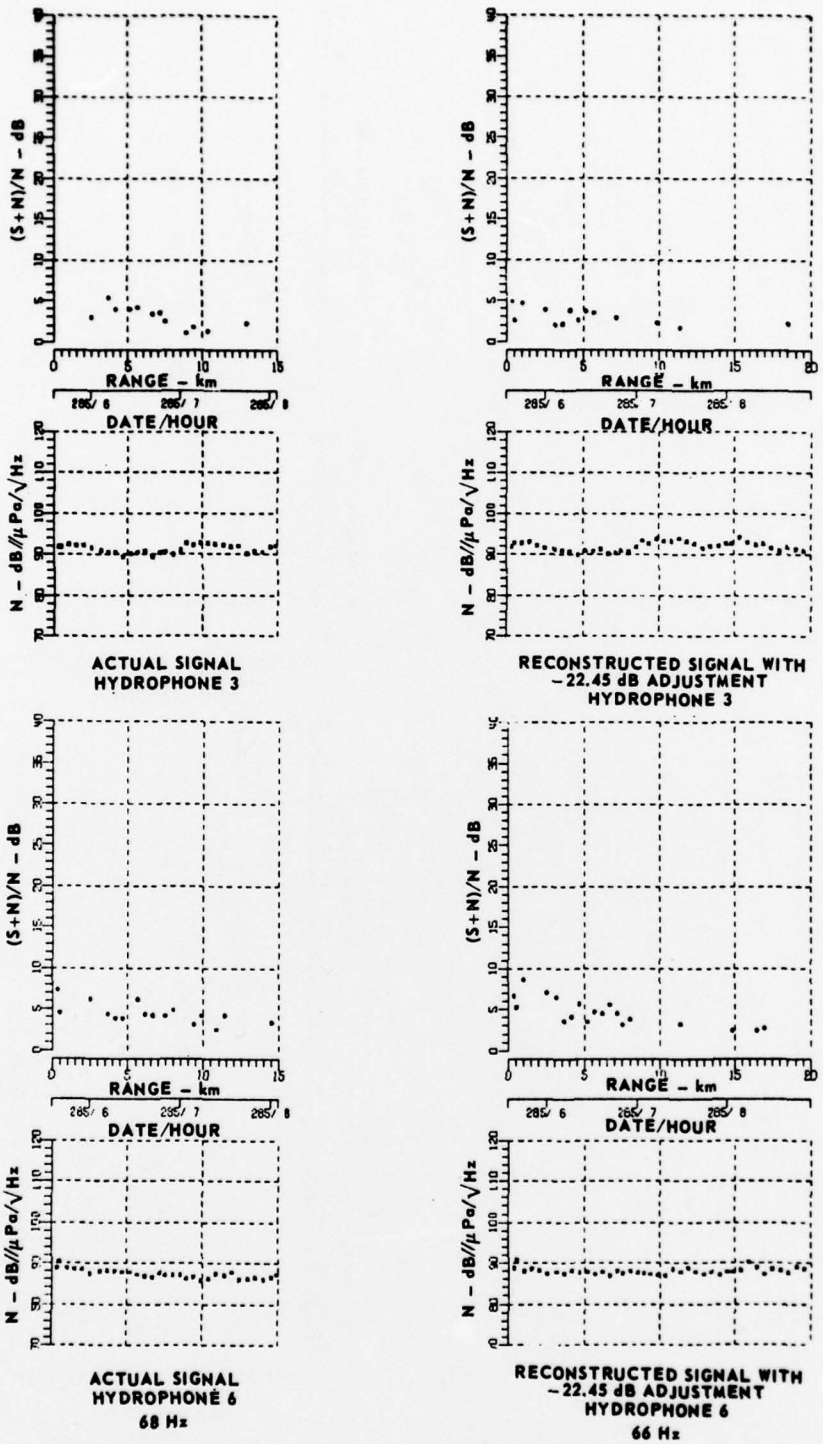

ARL:UT
AS-79-432
JAS-GA
3-20-79

FIGURE 6
SIGNAL EXCESS AND NOISE versus RANGE
FOR THE LOW FREQUENCIES OVER RUN 2

TABLE I

PERCENT OF SIGNAL DETECTIONS USING HYDROPHONE 3

	REAL 156 Hz	RECONSTRUCTED 166 Hz	REAL 68 Hz	RECONSTRUCTED 66 Hz
Run 1	45	74	--	--
Run 2	75	75	30	35

TABLE II

PERCENT OF SIGNAL DETECTIONS USING HYDROPHONE 6

	REAL 156 Hz	RECONSTRUCTED 166 Hz	REAL 68 Hz	RECONSTRUCTED 66 Hz
Run 1	58	74	--	--
Run 2	70	88	40	48

signal excess curves by about the 0.5 dB increment. The small shifts in this case were not enough to change the detection statistics. This does show that fine tuning adjustments can be made in the signal excess and that proper scaling is necessary.

REFERENCES

1. A. J. Perrone and L. A. King, "Analysis technique for classifying wind and ship-generated noise characteristics," J. Acoust. Soc. Am. 58, 1186-1189 (1975).

2. H. P. Bucker, "Cross sensor beamforming with a sparse line array," J. Acoust. Soc. Am. 61, 494-498 (1977)

DISTRIBUTION LIST FOR
ARL-TM-79-3
UNDER CONTRACT N00039-78-C-0307
UNCLASSIFIED

Copy No.

Commander
Naval Electronic Systems Command
Department of the Navy
Washington, DC 20360
1 Attn: PME-124
2- 4 PME-124/30
5 PME-124/40
6 PME-124/60
7 PME-124TA

Assistant Director of the Navy (RE&S)
Washington, DC 20301
8 Attn: G.A. Cann

Chief of Naval Operations
Department of the Navy
Washington, DC 20350
9 Attn: OP-095
10 OP-951
11 OP-955

Chief of Naval Development
Headquarters, Naval Material Command
Washington, DC 20360
12 Attn: MAT-035

Commander
Naval Air Development Center
Department of the Navy
Warminster, PA 18974
13 Attn: Code 205
14 Code 2052
15 Code 2055
16 Code 20P1
17 Code 2604
18 Code 602

19 Chief of Naval Research
Department of the Navy
Arlington, VA 22217

20 Commanding Officer
Naval Research Laboratory
Washington, DC 20375
21 Attn: Code 8100
22 Code 8160

Copy No.

23 Oceanographer of the Navy
Hoffman Building II
200 Stovall Street
Alexandria, VA 22332

Commander
Naval Air Systems Command
Department of the Navy
Washington, DC 20360
24 Attn: PMA-264

25 Commander
Naval Sea Systems Command
Department of the Navy
Washington, DC 20362
26 Attn: Code-06H1

27 Commander
Naval Ocean Systems Center
San Diego, CA 92152
28 Attn: M.R. Akers
29 Dr. R.A. Wagstaff
30 Dr. R.R. Gardner

31 Commander
Naval Surface Weapons Center
White Oak Laboratory
8121 Georgia Avenue
Silver Spring, MD 20910

32 Commander
New London Laboratory
Naval Underwater Systems Center
New London, CT 06320

Commander
Naval Oceanographic Office
Department of the Navy
NSTL Station, MS 39529
33 Attn: W. Geddes

Commanding Officer
Naval Intelligence Support Center
4301 Suitland Road
Washington, DC 20390
34 Attn: Code 222

Copy No.

35 Commanding Officer
Naval Ocean Research and Development Activity
NSTL Station, MS 39529
36 Attn: Code 320
37 Code 340
38 Code 500
39 Code 600

Defense Advanced Research Projects Agency
1400 Wilson Boulevard
Arlington, VA 22209
40 Attn: Dr. T. Kooij

ARPA Research Center
Unit 1, Bldg. 301A
NAS Moffett Field, CA 94035
41 Attn: E.L. Smith

42 Superintendent
Naval Postgraduate School
Monterey, CA 93940

Antisubmarine Warfare Systems Project Office
Department of the Navy
Washington, DC 20360
43 Attn: PM-4

44-53 Commanding Officer and Director
Defense Documentation Center
Defense Services Administration
Cameron Station, Building 5
5010 Duke Street
Alexandria, VA 22314

Applied Physics Laboratory
The Johns Hopkins University
The Johns Hopkins Road
Laurel, MD 20910
54 Attn: Dr. G.L. Smith

55 Applied Physics Laboratory
The University of Washington
1013 NE Fortieth Street
Seattle, WA 98195

Copy No.

Arthur D. Little, Inc.
Acorn Park
Cambridge, MA 02140
56 Attn: Dr. G.R. Raisbeck

57 Bolt, Beranek, and Newman, Inc.
1701 N. Fort Myer Drive
Arlington, VA 22209

58 Bell Telephone Laboratories
2 Whippany Road
Whippany, NJ 07981

Sanders Associates, Inc.
24 Simon Street
Nashua, NH 03060
59 Attn: L. Gagne

Scripps Institution of Oceanography at
The University of California, San Diego
La Jolla, CA 92093
60 Attn: V.C. Anderson

Planning Systems, Inc.
7900 Westpark Drive
McLean, VA 22101
61 Attn: Dr. R.L. Spooner

Science Applications, Inc.
8400 Westpark Drive
McLean, VA 22101
62 Attn: Dr. J.S. Hanna

Sutron Corporation
Suite 700
1925 N. Lynn Street
Arlington, VA 22209
63 Attn: C.H. Dabney

Tetra-Tech, Inc.
1911 N. Ft. Meyer Drive
Arlington, VA 22209
64 Attn: W.E. Sims

Copy No.

Tracor, Inc.
1601 Research Blvd.
Rockville, MD 20850
65 Attn: J.T. Gottwald

TRW, Inc.
TRW Defense & Space Systems Group
Washington Operation
7600 Colshire Drive
McLean, VA 22101
66 Attn: J. Bender

Underwater Systems, Inc.
World Building
8121 Georgia Avenue
Silver Spring, MD 20910
67 Attn: Dr. M.S. Weinstein

68 Western Electric Company
P.O. Box 20046
Greensboro, NC 27420

Woods Hole Oceanographic Institution
Woods Hole, MA 02543
69 Attn: E.E. Hays

70 Glen E. Ellis, ARL:UT

71 Loyd D. Hampton, ARL:UT

72 Kenneth E. Hawker, ARL:UT

73 Stephen K. Mitchell, ARL:UT

74 Clark S. Penrod, ARL:UT

75 Jack A. Shooter, ARL:UT

76 Reuben H. Wallace, ARL:UT

77 Library, ARL:UT

78-82 Reserve, ARL:UT